

Velocity-autocorrelation spectrum of simple classical liquids

J. Bosse, W. Götze, and Annette Zippelius

*Max-Planck-Institut für Physik und Astrophysik, D-8000 München, Germany
and Physik-Department der Technischen Universität München, 8046 Garching, Germany*

(Received 3 March 1978)

The velocity-autocorrelation function of a tagged particle moving in a classical liquid is expressed in terms of a characteristic oscillator frequency and a frequency-dependent relaxation kernel. The relaxation spectrum is approximated by calculating the interaction of the tagged particle with current excitations of the liquid. The interaction with the longitudinal modes is shown to be responsible for the observed peak structure of the correlation function. The results of the present theory, in particular the values for the diffusion constant, agree well with the molecular-dynamics experiments on argon and rubidium.

I. INTRODUCTION

The velocity-autocorrelation function $\psi(t)$ of classical liquids has been the subject of extensive theoretical studies in the past.¹ On the one hand, $\psi(t)$ is the simplest quantity describing the dynamics of a liquid. On the other hand, numerous computer simulations²⁻⁴ provide us with detailed experimental information on $\psi(t)$. As a function of time $\psi(t)$ shows a rapid initial decay, then it changes sign and approaches zero in a more or less oscillatory manner. The corresponding frequency spectrum, i.e., the Fourier transform $\psi''(\omega)$, exhibits a pronounced peak at nonzero frequency.

For the theory it remains to explain the position, height, and width of the resonance in $\psi''(\omega)$ and to calculate the zero-frequency limit $\psi''(0)$, which defines the self-diffusion constant D . A further point of interest has been the anomalous long-time behavior of $\psi(t)$. A tail proportional to $t^{-3/2}$ has been verified for a fluid of hard spheres⁵ as well as for soft repulsive potentials,⁶ while no long-time tails could be detected in the molecular dynamics data of liquid argon and liquid rubidium.²⁻⁴ Since it is known that the slow decay of hydrodynamic modes is responsible for these long-time singularities,^{7,8} any theory should incorporate the coupling between the tagged particle and the coherent modes of the liquid in an appropriate way.

Some of the early theoretical approaches⁹⁻¹¹ tried to explain the velocity-autocorrelation function of liquids in close analogy to $\psi(t)$ of solids. The itinerant oscillator model, e.g., proposed originally by Sears,¹⁰ emphasized the oscillatory component of the particle's motion. By introducing several fit parameters the improved version¹¹ of the model was able to reproduce the data on liquid argon quite well. Another line of approach is based on generalized Langevin equations for $\psi(t)$. Several authors¹² have tried phenomeno-

logical approximations for the relaxation kernels fixing the parameters with the aid of sum rules and the diffusion constant. It was even possible within this frame to estimate the diffusion constant.¹³ However, these calculations lead in a systematic fashion to resonances which are too narrow and have peak positions about twice as big as those in the experiments on liquid argon. This indicates that the resonance of $\psi''(\omega)$ cannot be explained on the basis of high-frequency asymptotics alone. A microscopic explanation going beyond sum rule arguments is required to fully understand $\psi(t)$. In another line of approach the tagged particle's current is identified with the coherent liquid excitations,¹⁴ which are taken from experiment or from hydrodynamic models, thereby introducing several fit parameters. In this way long-time tails may be included and the results agree qualitatively with experiment.

Mode-coupling theories have been worked out for the hard-core liquids¹⁵ to yield $\psi(t)$ in terms of decay integrals over the excitation spectra of the coherent liquid modes. The latter quantities were obtained by interpolation between the hydrodynamic and free gas limit, thereby introducing several phenomenological fit parameters.

In this paper the mode-coupling theory invented previously to study the coherent excitations of liquids¹⁶ will be used to calculate the spectrum of the velocity-autocorrelation function. It will be argued that the coupling of the self-motion to the collective longitudinal and transverse excitations is responsible for the observed features of $\psi''(\omega)$. Satisfactory quantitative agreement between our results and the experiments on liquid argon and liquid rubidium including the value of the diffusion constant D will be demonstrated.

The paper is organized as follows. First (Sec. II) a closed microscopic expression will be derived for the relaxation kernel entering the generalized Langevin equation making use of the formalism of

Zwanzig and Mori.^{17,18} In Sec. III the relaxation kernel is expressed in terms of two-mode decay integrals. The numerical results of argon and rubidium are presented in Sec. IV, and finally (Sec. V) some features of the present theory are discussed.

II. GENERALIZED LANGEVIN EQUATION

Let us consider a system of N classical particles of mass m in a volume V at temperature T . Position and velocity of the n th particle are denoted by \vec{r}_n and \vec{v}_n . Let us imagine the presence of a further tagged particle of mass m_0 with position $\vec{r}_0(t)$ and velocity $\vec{v}_0(t)$. The velocity-autocorrelation function is defined by

$$\begin{aligned} \psi(t) &= \frac{1}{3} \langle \vec{v}_0(t'+t) \cdot \vec{v}_0(t') \rangle \\ &= T \langle v_0^x | e^{-it\mathcal{L}} | v_0^x \rangle, \end{aligned} \quad (1)$$

with $\langle \rangle$ denoting the thermal average. The latter expression in Eq. (1) results from the introduction of a scalar product in the space of dynamical variables according to $\langle A|B \rangle = \langle \delta A^* \delta B \rangle / T$, with $\delta A = A - \langle A \rangle$ and of the Hermitian Liouville operator \mathcal{L} describing time evolution $A(t) = e^{it\mathcal{L}} A$; explicit use has also been made of the invariance of the system in space rotations and time translations.¹⁸

Calculations of correlation functions are best performed by starting from exact equations of motion and then approximating the relaxation kernels appearing in these equations. To generate such an equation of motion for $\psi(t)$ the identity¹⁷

$$\begin{aligned} \frac{d}{dt} e^{-it\mathcal{L}} &= -i\mathcal{L} \mathcal{O} e^{-it\mathcal{L}} - \int_0^t d\tau \mathcal{L} \mathcal{Q} e^{-i(t-\tau)\mathcal{Q}\mathcal{L}\mathcal{Q}} \mathcal{L} \mathcal{O} e^{-i\tau\mathcal{L}} \\ &\quad - i\mathcal{L} \mathcal{Q} e^{-it\mathcal{Q}\mathcal{L}\mathcal{Q}} \end{aligned} \quad (2)$$

for any projector \mathcal{O} and its complement $\mathcal{Q} = 1 - \mathcal{O}$ will be used. If \mathcal{O} denotes the projector onto the vector $|v_0^x\rangle$, differentiation of Eq. (1) will result in the generalized Langevin equation

$$\dot{\psi}(t) = - \int_0^t d\tau K(t-\tau) \psi(\tau), \quad (3a)$$

$$\psi(t=0) = T/m_0 = T \langle v_0^x | v_0^x \rangle,$$

with the memory function

$$K(t) = m_0 \langle \mathcal{L} v_0^x | e^{-it\mathcal{Q}\mathcal{L}\mathcal{Q}} | \mathcal{L} v_0^x \rangle. \quad (3b)$$

This is easily verified using the fact $\langle v_0^x | \mathcal{L} | v_0^x \rangle = 0$, which is a consequence of the above-mentioned stationarity property $\langle \dot{v}_0^x v_0^x \rangle = 0$. For the memory function $K(t)$ a similar equation of motion will result with the aid of Eq. (2), if \mathcal{O}' denotes the

projector onto the "force" $|\mathcal{L} v_0^x\rangle$ and \mathcal{L} is replaced by $\mathcal{Q}\mathcal{L}\mathcal{Q}$:

$$\begin{aligned} \dot{K}(t) &= - \int_0^t d\tau M(t-\tau) K(\tau), \\ K(t=0) &= \Omega_{E0}^2 = m_0 \langle v_0^x | \mathcal{L}^2 | v_0^x \rangle. \end{aligned} \quad (4a)$$

The relaxation kernel $M(t)$ is given by

$$M(t) = m_0 \langle \mathcal{Q} \mathcal{L}^2 v_0^x | e^{-it\mathcal{Q}'\mathcal{Q}\mathcal{L}\mathcal{Q}\mathcal{Q}'} | \mathcal{Q} \mathcal{L}^2 v_0^x \rangle / \Omega_{E0}^2. \quad (4b)$$

Combination of Eqs. (3a) and (4a) results in the exact equation of motion;

$$\ddot{\psi}(t) + \Omega_{E0}^2 \psi(t) + \int_0^t d\tau M(\tau) \dot{\psi}(t-\tau) = 0, \quad (5)$$

or, equivalently, in the spectrum of the velocity autocorrelation;

$$\begin{aligned} \psi''(\omega) &= \frac{1}{2} \int_{-\infty}^{+\infty} dt e^{it\omega} \frac{\psi(t)}{T} \\ &= \frac{\Omega_{E0}^2}{m_0} \frac{M''(\omega)}{[\omega^2 - \Omega_{E0}^2 + \omega M'(\omega)]^2 + [\omega M''(\omega)]^2}. \end{aligned} \quad (6a)$$

Here $M''(\omega)$ and $M'(\omega)$ are, respectively, the absorptive and the dispersive part of the relaxation spectrum;

$$\begin{aligned} M''(\omega) &= \frac{1}{2} \int_{-\infty}^{+\infty} dt e^{it\omega} M(t), \\ M'(\omega) &= \frac{PP}{\pi} \int_{-\infty}^{+\infty} d\epsilon \frac{M''(\epsilon)}{\epsilon - \omega}. \end{aligned} \quad (6b)$$

For the spectrum $K''(\omega)$ of the memory function (3b) one has from (4a)

$$\begin{aligned} K''(\omega) &= \frac{1}{2} \int_{-\infty}^{+\infty} dt e^{it\omega} K(t) \\ &= \Omega_{E0}^2 \frac{M''(\omega)}{[\omega + M'(\omega)]^2 + [M''(\omega)]^2}. \end{aligned} \quad (6c)$$

In view of Eq. (5) the spectral function (6a) can be interpreted¹⁹ as the response function of a damped harmonic oscillator. $M''(\omega)$ is the generalized friction coefficient; it describes the decay of oscillation with frequency Ω_{E0} into the incoherent many-particle excitations. The frequency variation of $M''(\omega)$ leads to a nontrivial renormalization $\omega M'(\omega)$ of the oscillator frequency.

The mathematical framework formulated above is very general and has been used extensively in the preceding literature. The results of Berne *et al.*¹² on the velocity-autocorrelation function, e.g., are obtained by setting $M''(\omega)$ constant and determining this constant from the self-diffusion coefficient D according to the relation

$$D = \int_0^\infty dt \psi(t) = T\psi''(\omega=0) = \frac{T}{m_0} \frac{M''(\omega=0)}{\Omega_{E0}^2}. \quad (7)$$

The motion of the tagged particle is determined by Newton's equations;

$$\dot{r}_0^\alpha(t) = v_0^\alpha(t), \quad \alpha = x, y, z, \quad (8a)$$

$$\dot{v}_0^\alpha = -\frac{1}{m_0} \sum_{n=1}^N \frac{\partial}{\partial r_0^\alpha} u_0(|\vec{r}_0 - \vec{r}_n|), \quad (8b)$$

with the potential $u_0(r)$ between the fluid particles and the tagged one. Introducing Fourier transforms of the potential and the particle densities and the particle current densities,

$$\rho_0(\vec{k}) = e^{-i\vec{k} \cdot \vec{r}_0}, \quad \rho(\vec{k}) = \sum_n e^{-i\vec{k} \cdot \vec{r}_n}, \quad (9a)$$

$$\vec{j}_0(\vec{k}) = \vec{v}_0 e^{-i\vec{k} \cdot \vec{r}_0}, \quad \vec{j}(\vec{k}) = \sum_n \vec{v}_n e^{-i\vec{k} \cdot \vec{r}_n}, \quad (9b)$$

Eq. (8a) may be rewritten as the continuity equation for the tagged particle

$$\mathcal{L}\rho_0(\vec{k}) = -\vec{k} \cdot \vec{j}_0(\vec{k}), \quad (10a)$$

while Eq. (8b) becomes

$$\mathcal{L}v_0^\alpha = -\frac{1}{m_0} \int \frac{d^3k}{(2\pi)^3} u_0(k) k^\alpha \rho_0(-\vec{k}) \rho(\vec{k}). \quad (10b)$$

Applying \mathcal{L} to this latter equation and using the continuity equations for $\rho(\vec{k})$ and $\rho_0(\vec{k})$ one im-

mediately arrives at

$$\mathcal{L}^2 v_0^\alpha = \frac{1}{m_0} \sum_\beta \int \frac{d^3k}{(2\pi)^3} u_0(k) k^\alpha k^\beta [\rho_0(-\vec{k}) \vec{j}^\beta(\vec{k}) - \vec{j}_0^\beta(-\vec{k}) \rho(\vec{k})]. \quad (11)$$

Finally, Eq. (11) may be used in the definition equation (4a) to express Ω_{E0}^2 , which is related to the second frequency moment of the velocity autocorrelation spectrum, as

$$\begin{aligned} \Omega_{E0}^2 &= m_0 \int_{-\infty}^{+\infty} \frac{d\omega}{\pi} \omega^2 \psi''(\omega) \\ &= \frac{-\ddot{\psi}(t=0)}{\psi(t=0)} \\ &= \frac{1}{m_0} \frac{1}{3} \frac{N}{V} \int d^3r g_0(r) \Delta u_0(r), \end{aligned} \quad (12)$$

where $g_0(r)N/V = \langle \sum_n \delta(\vec{r} - \vec{r}_0 + \vec{r}_n) \rangle$ is the pair-correlation function.²⁰ Ω_{E0} will be the frequency of the tagged particle treated in harmonic approximation, if all the other particles' positions are fixed in space.

III. MODE-COUPLING APPROXIMATION

Within the mode-coupling theory¹⁶ one approximates the matrix element Eq. (4b) by inserting the simplest product states and factorizing their correlations. Thus we write for $M(t)$

$$\begin{aligned} M(t) &\simeq \frac{m_0}{\Omega_{E0}^2} \sum_{\vec{k}, \alpha, \beta} (Q \mathcal{L}^2 v_0^\alpha | \rho_0(\vec{k}) j^\alpha(-\vec{k}) \{ (j^\alpha(-\vec{k}) | j^\alpha(-\vec{k})) T(\rho_0(\vec{k}) | \rho_0(\vec{k})) \}^{-1} \\ &\quad \times (\rho_0(\vec{k}, t) | \rho_0(\vec{k})) T(j^\alpha(-\vec{k}, t) | j^\beta(-\vec{k})) \{ (j^\beta(-\vec{k}) | j^\beta(-\vec{k})) T(\rho_0(\vec{k}) | \rho_0(\vec{k})) \}^{-1} \\ &\quad \times (\rho_0(\vec{k}) | j^\beta(-\vec{k}) | Q \mathcal{L}^2 v_0^\alpha \}. \end{aligned} \quad (13)$$

In writing Eq. (13) all intermediate states but $\rho_0(\vec{k}) j^\alpha(-\vec{k})$ were neglected and the motion of those pair modes was assumed to be independent. One of the intermediate modes in Eq. (13) is given by the density autocorrelation function

$$\begin{aligned} \phi_0(k, t) &= T(\rho_0(\vec{k}, t) | \rho_0(\vec{k})) \\ &= \langle \exp[-i\vec{k} \cdot (\vec{r}_0(t) - \vec{r}_0)] \rangle. \end{aligned} \quad (14)$$

The second intermediate mode is the current propagator, which will be represented in terms of the coherent longitudinal and transverse current-excitation spectra $\phi_{L,T}''(k, \omega)$;

$$\begin{aligned} \phi_{\alpha\beta}(\vec{k}, t) &= \frac{(j^\alpha(\vec{k}, t) | j^\beta(\vec{k}))}{(j^\alpha(\vec{k}) | j^\alpha(\vec{k}))} \\ &= \int_{-\infty}^{+\infty} \frac{d\omega}{\pi} e^{-it\omega} \\ &\quad \times \left[\frac{k^\alpha k^\beta}{k^2} \phi_L''(k; \omega) \right. \\ &\quad \left. + \left(\delta_{\alpha\beta} - \frac{k^\alpha k^\beta}{k^2} \right) \phi_T''(k, \omega) \right]. \end{aligned} \quad (15)$$

The vertex entering in Eq. (13) can be worked out

with the aid of Eq. (11). Introducing the dimensionless function $V_{\alpha\beta}(\vec{k})$ according to

$$\begin{aligned} V_{\alpha\beta}(\vec{k}) &= -\frac{m}{\Omega_{E0}^2} (Q\mathcal{L}^2 v_0^\alpha | \rho_0(\vec{k}) j^\beta(-\vec{k}) \\ &= \frac{N/V}{m_0 \Omega_{E0}^2} \int d^3r e^{-i\vec{k}\cdot\vec{r}} g_0(\vec{r}) \nabla_\alpha \nabla_\beta u_0(\vec{r}), \end{aligned} \quad (16)$$

one finds that these quantities approach 1 as $k \rightarrow 0$ according to Eq. (12). Substituting the expres-

sions (14)–(16) in Eq. (13) leads to

$$M(t) = 2M_T(t) + M_L(t), \quad (17a)$$

$$\begin{aligned} M_{T,L}(t) &= \frac{m_0}{m} \frac{\Omega_{E0}^2}{N/V} \frac{1}{6\pi^2} \int_0^\infty dk k^2 V_{T,L}^2(k) \phi_0(k; t) \\ &\quad \times \phi_{T,L}(k; t), \end{aligned} \quad (17b)$$

where $V_T(k) = V_{xx}(k)$ and $V_L(k) = V_{zz}(k)$ if the z axis points in k direction. According to Eq. (6b) we get for the transverse and longitudinal contributions to the relaxation spectrum

$$M_{T,L}''(\omega) = \frac{m_0}{m} \frac{\Omega_{E0}^2}{N/V} \frac{1}{6\pi^2} \int_0^\infty dk k^2 V_{T,L}^2(k) \int_{-\infty}^{+\infty} \frac{d\epsilon}{\pi} \phi_0''(k, \epsilon) \phi_{T,L}''(k, \omega - \epsilon). \quad (17c)$$

For the incoherent density correlation $\phi_0(k, t)$ we exploit the Gauss approximation, which yields $\phi_0(k, t)$ in terms of $\psi(t)$;

$$\phi_0(k, t) \simeq \exp\left(-k^2 \int_0^t d\tau (t - \tau) \psi(\tau)\right). \quad (18)$$

This approximation is known to be exact in the free gas as well as in the hydrodynamic regime. For intermediate times it deviates up to 20% from the exact result.²¹

The coherent current fluctuation spectra are taken from our preceding work,^{16,22,23} which provided a microscopic theory for $\phi_{T,L}''(k, \omega)$.

In the approximation of the relaxation kernel one might consider other decay processes, namely, the decay into a coherent density and the tagged particle's current, which according to Eq. (11) has a nonzero overlap with the fluctuating force $Q\mathcal{L}^2 v_0^\alpha$. The corresponding vertex function would involve higher-order static correlations; i.e., the triplet correlation function $g_3(\vec{r}; \vec{r}')$. In the present work we restricted, however, to the simplest decays discussed above.

IV. RESULTS FOR LIQUID ARGON AND LIQUID RUBIDIUM

The preceding theory has been worked out numerically for liquid argon and liquid rubidium. The input parameters were chosen to agree with those used in Rahman's molecular dynamics work.^{2,3} Argon is considered for $T = 85^\circ\text{K}$ at a density $n = 2.14 \times 10^{22} \text{ cm}^{-3}$ ($m = 66.3 \times 10^{-24} \text{ g}$); rubidium is considered for $T = 319^\circ\text{K}$ at a density $n = 1.06 \times 10^{22} \text{ cm}^{-3}$ ($m = 141.9 \times 10^{-24} \text{ g}$). The tagged particle is chosen to be identical with the system's particles, hence $m_0 = m$ in the preceding formulas, while $u_0(\vec{r}) = v(\vec{r})$ and $g_0(\vec{r}) = g(\vec{r})$ are the system's pair potential and pair-correlation function, respectively. The latter are taken from Rahman's work^{3,24} for liquid Rb and from the measurements of Wentzel, Yarnell, and Katz²⁵ for liquid Ar. These data determine the Einstein frequency [Eq. (12)]; $\Omega_E = 0.78 \times 10^{13} \text{ sec}^{-1}$ in the case of argon; $\Omega_E = 0.61 \times 10^{13} \text{ sec}^{-1}$ for rubidium.

The normalized vertex functions $V_L(k)$ and $V_T(k)$ [Eq. (16)] were calculated from the above data and are plotted in Fig. 1.

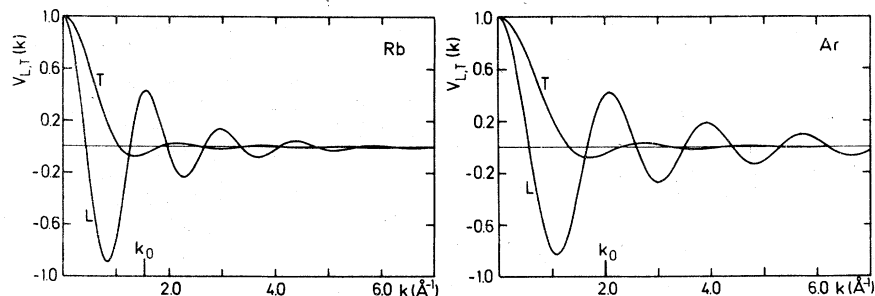


FIG. 1. Normalized vertex functions $V_L(k)$ and $V_T(k)$ according to Eq. (16).

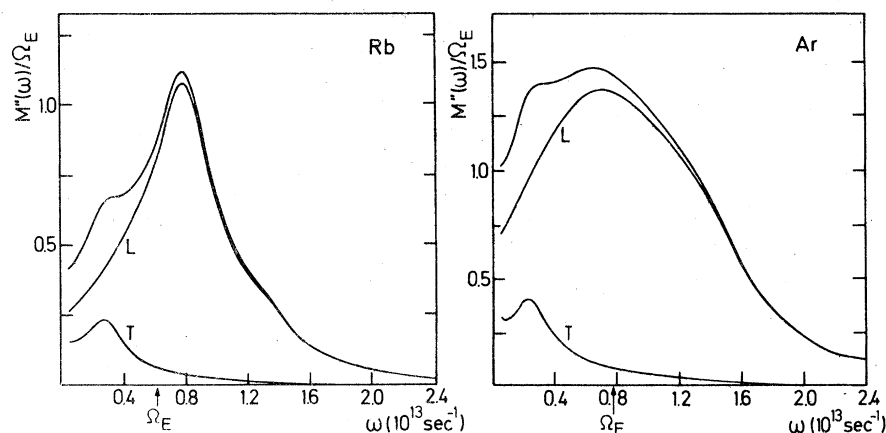


FIG. 2. Relaxation spectra $M''(\omega)/\Omega_E$. The transverse and longitudinal contributions are denoted by $T \equiv 2M''_T(\omega)/\Omega_E$ and $L \equiv M''_L(\omega)/\Omega_E$, respectively.

The nonlinear mode-coupling equations of Sec. III can be solved by iteration as discussed in our earlier work.^{16,22} The calculated relaxation spectra are presented in Fig. 2. Quite similar to the relaxation spectra of the coherent functions^{22,23} $M''(\omega)$ exhibits a maximum around the characteristic frequency Ω_E ; it drops off rather steeply for frequencies around $2\Omega_E$, and it shows a pronounced minimum for small ω .

In Fig. 3 the generalized friction spectrum $K''(\omega)$ [Eq. (6c)] is presented. Similar to the dynamical transport coefficients worked out previously for the coherent current-correlation functions it consists of a narrow low-frequency peak situated on a plateau. The experimental curve for $K''(\omega)$ shown in the figure is obtained from Rahman's $\psi(t)$ data by inverting Eq. (3a). The dotted curve is the Lorentzian obtained from (6c), when replacing $M''(\omega)$ by a constant chosen to fit the experimental diffusion constant D

[Eq. (7)].

Figure 4 shows the final result for the velocity-autocorrelation spectrum of a tagged particle $\psi''(\omega)$ in comparison with Rahman's data.^{2,3} Also shown is the semiphenomenological curve of Berne *et al.*¹² for liquid argon; their approximation has also been evaluated for liquid rubidium and included in Fig. 4. The numerical values for the diffusion constants of the present theory [Eq. (7)] are $D = 2.2 \times 10^{-5} \text{ cm}^2 \text{ sec}^{-1}$ for Ar and $D = 2.1 \times 10^{-5} \text{ cm}^2 \text{ sec}^{-1}$ for Rb in comparison with the experimental values $D_{\text{expt}} = 1.9 \times 10^{-5} \text{ cm}^2 \text{ sec}^{-1}$ for Ar,² and $D_{\text{expt}} = 2.4 \times 10^{-5} \text{ cm}^2 \text{ sec}^{-1}$ for Rb.³

The experimental spectrum exhibits a peak at about $\frac{1}{2}\Omega_E$ for Ar and at about Ω_E for Rb; this peak position is reproduced by the present theory. However, the theoretical peak is somewhat narrower than the experimental one, and the theory yields shoulders in the spectrum at about $2\Omega_E$ which are not present in the experiment.

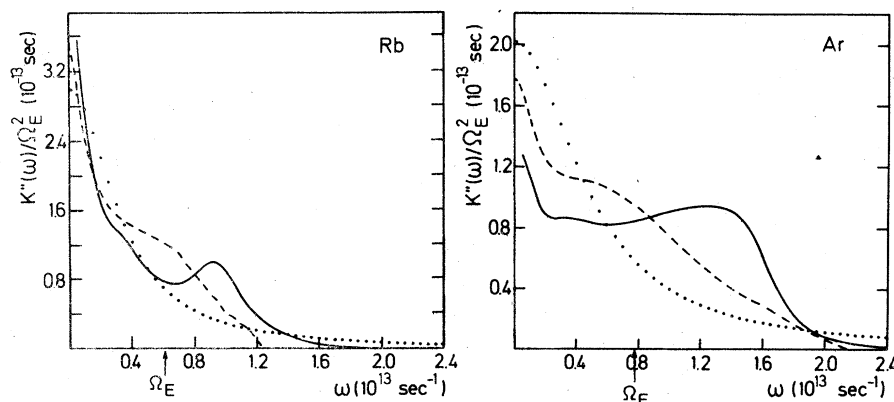


FIG. 3. Friction spectra $K''(\omega)/\Omega_E^2$ of the present theory (full curve) compared to the spectra, derived from Rahman's data (Refs. 2 and 3) (dashed curve). The dotted line shows the single relaxation approximation (Ref. 23) with the experimental value for D .

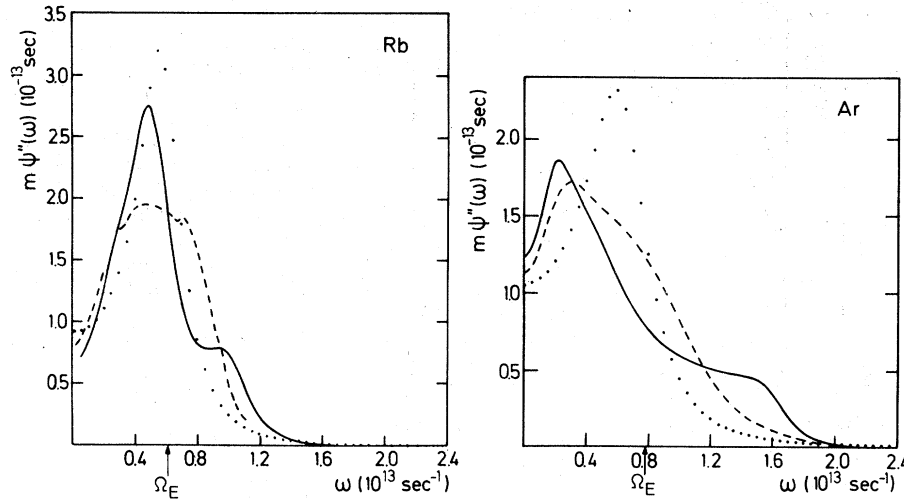


FIG. 4. Velocity auto-correlation spectrum $\psi''(\omega)$ of the present theory (full curves) in comparison with Rahman's molecular dynamics data (Refs. 2 and 3) (dashed curve) and the single relaxation approximation (Ref. 12) (dotted curve).

V. DISCUSSION

A. Relaxation and mode decay

The absorptive part of the relaxation kernel is given by the golden-rule type of expression (17). The coherent state of the tagged particle changes due to emission and absorption of excitations of the liquid. In leading order only single current modes of momentum \vec{k} are considered, transferring the recoil $-\vec{k}$ to the particle. The coupling of the tagged particle to the liquid is given by the vertex functions $V_{\alpha\beta}(\vec{k})$; according to Eq. (16) this quantity can be viewed as the averaged dynamical matrix of the system. Convergence of the decay integrals (17c) is ensured by the decrease of the vertex $V(k)$ with increasing momentum. As usual in systems with regular interactions the coupling will become ineffective, if the momenta are too large. It is plausible, and it is obvious from Eq. (16) or Fig. 1 that the coupling V_L to longitudinal modes is more effective for large momenta than the coupling V_T to transverse modes, i.e., the coupling to shear excitations.

The present theory ignores all but the simplest decay processes. From the theory of the auto-correlation function in lattices the decay into more phonon states is known to give smooth contributions to $\psi''(\omega)$ which may be important for large frequencies. So we must expect the present theory to underestimate $M''(\omega)$ for $\omega > 2\Omega_E$. Thus, to the same extent the sharp high-frequency cutoff in $M_L''(\omega)$ (see Fig. 2) seems to be an artifact of the present theory. This sharp cutoff, however, via Eq. (6b) produces a large $M'(\omega)$ which in turn leads to the high-frequency bump in $K''(\omega)$ and the shoulders in $\psi''(\omega)$ via Eqs. (6c) and (6a), respectively. Even though one might question the

reliability of the experimental data for $\psi''(\omega)$ or $K''(\omega)$ in the frequency range $\omega > 2\Omega_E$, the discrepancy between experiment and theory in this regime is presumably due to our neglect of more complicated decay channels.

B. Longitudinal versus transverse decay

Since the excitation spectrum of longitudinal modes in liquids is quite different from the excitation spectrum of transverse modes, it is obvious that the contribution $M_T''(\omega)$ differs considerably from the contribution $M_L''(\omega)$. Introducing a generalized damping function $D_T''(k, \omega)$,²⁶ the transverse spectrum becomes

$$\phi_T''(k, \omega) = \frac{k^2 D_T''}{(\omega + k^2 D_T')^2 + (k^2 D_T'')^2}, \quad (19a)$$

where D_T' is connected to D_T'' via a Kramers-Kronig dispersion relation similar to Eq. (6b).

In the hydrodynamic limit ($q, \omega \rightarrow 0$, $D_T' \rightarrow \eta/(nm)$, and $D_T'' \rightarrow 0$). The longitudinal spectrum, on the other hand, reads²⁶

$$\phi_L''(k, \omega) = \frac{\omega^2 k^2 D_L''}{(\omega^2 - c^2 k^2 + \omega k^2 D_L')^2 + (\omega k^2 D_L'')^2}, \quad (19b)$$

with c denoting the k -dependent sound velocity and $D_L''(k, \omega)$ abbreviating a generalized sound-damping function; in the hydrodynamic limit $D_L'' \rightarrow \Gamma$, $D_L' \rightarrow 0$.

One can split the k integral for $M_T''(\omega)$ in Eq. (17c) into three regimes. First let $k/k_0 > 0.75$, where k_0 denotes the peak position of the liquid structure factor $S(k)$; $k_0 \sim 2.0 \text{ \AA}^{-1}$ for Ar, $k_0 \sim 1.5 \text{ \AA}^{-1}$ for Rb. Then $\phi_T''(k, \omega)$, essentially, is a structureless k -independent function decreasing with increasing ω .^{22, 23} Hence the corresponding

contribution to $M_T''(\omega)$ is a smoothly decreasing function; this part is explicitly visible in Fig. 2 for $\omega > \frac{1}{2}\Omega_E$. Second, for $0.15 < k/k_0 < 0.75$, $\phi_T''(k, \omega)$ shows a shear-mode resonance at a frequency $\omega_T(k)$ which increases with momentum k .^{22,23} With increasing ω , $\phi_0''(k, \omega)$ picks up larger and larger k values, so that the increasing phase space for shear modes yields an increasing contribution to $M_T''(\omega)$; this increase is responsible for the maximum of $M_T''(\omega)$ in Fig. 2. Third, for still smaller wave numbers $k/k_0 < 0.15$, a well-defined shear mode ceases to exist and the transverse correlation shows hydrodynamic diffusive behavior. The diffusion propagator is a decreasing function of frequency and hence it yields a decreasing contribution for $M_T''(\omega)$ for small ω and this explains the low-frequency minimum of $M_T''(\omega)$ visible in Fig. 2 for Ar. Actually, the diffusion propagator yields a singular function proportional to $-\sqrt{\omega}$. This singularity at small frequencies is responsible for the well-known long-time tail^{7,8} of $\psi(t) = (T/12mn)[\pi t(D+D_T)]^{3/2}$, which is correctly included in the present approximation.

The longitudinal propagator [Eq. (19b)] vanishes for $\omega \rightarrow 0$ independent of the value of k ; this is due to the conservation of particle number. Thus $M_L''(\omega)$ should be zero for $\omega \rightarrow 0$, if $\phi_0''(k, \epsilon)$ were a $\delta(\epsilon)$ function. This is not the case, however, since the wave-absorption process has inelastic components. Therefore $M_L''(\omega \rightarrow 0) \neq 0$, and according to Fig. 2 the zero-frequency contribution of the longitudinal channel is even larger than the one of the transverse channel.

The prominent feature of the longitudinal part of $M''(\omega)$ is, however, its strong increase with increasing ω . This is not solely due to the ω^2 factor in Eq. (19b). For larger values of ω and k , $\phi_L''(k, \omega)$ behaves like a normalized broadened-resonance function exhibiting a peak at $\omega = \omega_L(q)$. The longitudinal dispersion law $\omega_L(q)$ shows the typical maximum-minimum behavior^{22,23} of liquid spectra, and so a large phase space is picked up in the decay integral (17c) around $\omega \sim \Omega_E$. Hence, the maximum and the deep low-frequency hole of $M_L''(\omega)$ are a consequence of the kinematics ruling the tagged particle's density-wave emission and absorption.

$M_L''(\omega)$ dominates the relaxation spectrum $M''(\omega)$. The interesting small low-frequency peak of $M_T''(\omega)$ is compensated in its effect by the strong increase of $M_L''(\omega)$ for $\omega > 0.05 \times 10^{13} \text{ sec}^{-1}$. The increase of $M''(\omega)$ with increasing ω due to opening of the longitudinal decay channel leads to the pronounced non-Lorentzian form of the friction spectrum $K''(\omega)$. This frequency spectrum is responsible for the shift of the peak in $\psi''(\omega)$ from the value Ω_E down to lower values (Fig. 4).

From the preceding discussion one concludes that the observed peak position of $\psi''(\omega)$ can be understood as a result of the nonwhite relaxation spectrum $M''(\omega)$. The structure of $M''(\omega)$ is due to the tagged particle emitting and absorbing density fluctuations. The tagged particle's friction, i.e., its coupling to the liquid shear motion, is relevant for getting the correct numerical value for the diffusion constant.

Finally, one might try to improve the approximation of Berne *et al.*¹² by using a representation for the relaxation kernel $M''(\omega)$ which is analogous to Eq. (6c),

$$M''(\omega) = M(t=0) \frac{N''(\omega)}{[\omega + N'(\omega)]^2 + [N''(\omega)]^2},$$

and then replacing $N''(\omega)$ by a constant. Using Rahman's value² for the fourth moment of $\psi''(\omega)$ we evaluated the corresponding frequency spectrum of argon. The resulting $\psi''(\omega)$ shows no serious improvement over the approximation of Berne *et al.*¹² demonstrating that high-frequency asymptotics cannot provide an explanation of the observed peak structure. The value of $M(t=0)$ calculated in the mode-coupling approximation deviates by about 30% from Rahman's data.

C. Liquid argon versus liquid rubidium

There are three striking differences between the relaxation kernels of argon and rubidium (Fig. 2). First, the zero-frequency value of M''/Ω_E in Ar is more than twice the corresponding value in Rb. Second, the maximum of $M''(\omega)$ is somewhat higher and much broader in argon than in rubidium. Third, while $M''(\omega)$ has its peak at about Ω_E in argon it is located at about $1.5 \Omega_E$ in rubidium. These differences together imply the minimum of $M''(\omega)$ for $\omega < \Omega_E$ to be more pronounced in Rb than in Ar. Since the vertices (Fig. 1) for argon are only slightly bigger and slightly more extended in k space (after scaling with k_0) than in rubidium the mentioned differences have to be traced back to the differences in the structure of the coherent excitations of the two liquids.

In general the longitudinal dispersion curve $\omega_L(q)$ is steeper in Rb than in Ar; in particular, the sound velocity is higher in Rb than in Ar. Hence the low-frequency density of states is smaller in Rb than in Ar. This explains why $M_L''(\omega)$ is smaller and flatter for $\omega \ll \Omega_E$ in Rb than in Ar. As a result the properly scaled diffusion constant Dk_0^2/Ω_E is smaller in Rb than in Ar. Consequently the properly scaled $\phi_0''(k, \omega)$ is sharper in Rb than in Ar and this leads to a further decrease of $M_L''(\omega \rightarrow 0)$ in Rb relative to Ar. The difference of $Dk_0^2/$

Ω_E explains also why $M''(\omega)$ is smaller in Rb than in Ar. So the larger stiffness constant of Rb is responsible for a reduced value of $M''(0)/\Omega_E$, this effect being enhanced in a consistent way by a small value of the effective diffusion constant in liquid Rb.

Since the dispersion curve $\omega_L(q)$, in particular in the maxon-roton regime $q \sim \frac{1}{2}k_0$ and $q \sim k_0$,^{22,23} is considerably flatter in Ar than in Rb the density of longitudinal states for $\Omega \sim \Omega_E$ is larger in Ar than in Rb. Since Dk_0^2 is bigger in argon than in Rb the density of states $\int \phi_L''(k, \omega) dk$ is smeared out much more due to the convolution, Eq. (17c). The longitudinal frequencies $\omega_L(q)/\Omega_E$ are larger in Rb than in Ar for $q \sim \frac{1}{2}k_0$ and for $q > k_0$ and this explains why $M''_L(\omega)$, in particular its maximum, is located at higher frequencies in Rb than in Ar. So the different density of longitudinal states for both liquids yields the differences in peak position and height of $M''(\omega)$.

The peak of $\psi''(\omega)$, Fig. 4, is due to level repulsion between the coherent oscillator with resonance Ω_E and the pair excitations whose resonance is represented by the maximum of $M''(\omega)$. The level repulsion is less effective in Rb than in Ar, since $M''(\omega)$ is smaller and since the resonance position is higher in Rb than in Ar. This level repulsion thus explains the shift of the resonance of Ar down to $\frac{1}{2}\Omega_E$ while the resonance in Rb is shifted only slightly below Ω_E . The most remarkable feature of $\psi''(\omega)$, i.e., the appearance of a resonance at about $\frac{1}{2}\Omega_E$, thus is explained by the present theory due to hybridization of the coherent oscillator motion with the pair excitations of the liquid.

ACKNOWLEDGMENTS

Discussions with Dr. M. Lücke are gratefully acknowledged. We also thank Professor A. Rahman for sending us some of his original data.

- ¹K. S. Singwi and A. Sjölander, *Phys. Rev.* **167**, 152 (1968); N. Corngold and J. J. Duderstadt, *Phys. Rev. A* **2**, 836 (1970); T. G. Gaskell, *J. Phys. C* **4**, 1466 (1971); M. J. Barker and T. G. Gaskell, *J. Phys. C* **5**, 353 (1972); S. K. Mitra, *J. Phys. C* **6**, 801 (1973).
- ²A. Rahman, *Phys. Rev.* **136**, A405 (1964).
- ³A. Rahman (private communication).
- ⁴W. Schommers, *Solid State Commun.* **6**, 45 (1975).
- ⁵B. J. Alder and T. E. Wainwright, *Phys. Rev. Lett.* **18**, 988 (1967).
- ⁶D. Levesque and W. T. Ashurst, *Phys. Rev. Lett.* **33**, 277 (1974).
- ⁷Y. Pomeau and P. Résibois, *Phys. Rep.* **19C**, 64 (1975).
- ⁸M. A. Ernst and J. R. Dorfman, *J. Stat. Phys.* **12**, 311 (1975).
- ⁹A. Rahman, K. S. Singwi, and A. Sjölander, *Phys. Rev.* **126**, 997 (1962).
- ¹⁰V. F. Sears, *Proc. Phys. Soc. Lond.* **86**, 953 (1965).
- ¹¹Y. Nakahara and H. Takahashi, *Proc. Phys. Soc. Lond.* **89**, 747 (1966); P. S. Damle, A. Sjölander, and K. S. Singwi, *Phys. Rev.* **165**, 277 (1968).
- ¹²B. J. Berne, J. P. Boon, and S. A. Rice, *J. Chem. Phys.* **45**, 1086 (1966); K. S. Singwi and M. O. Tosi, *Phys. Rev.* **157**, 153 (1967); R. C. Desai and S. Yip, *ibid.* **166**, 129 (1968); D. Levesque and L. Verlet, *Phys. Rev. A* **2**, 2514 (1970).
- ¹³P. C. Martin and S. Yip, *Phys. Rev.* **170**, 151 (1968).
- ¹⁴B. J. Alder and T. E. Wainwright, *Phys. Rev. A* **1**, 18 (1970); Robert Zwanzig and Mordechai Bixon, *Phys. Rev. A* **2**, 2005 (1970); T. Geszti and J. Ker-tesz (unpublished); Toyonori Munakata and Akito Igarashi, *Prog. Theor. Phys.* **58**, 1345 (1977).
- ¹⁵P. Résibois and J. L. Lebowitz, *J. Stat. Phys.* **12**, 483 (1975); P. Résibois, *ibid.* **13**, 393 (1975); P. M. Furta-
do, G. F. Mazenko, and S. Yip, *Phys. Rev. A* **14**, 869 (1976).
- ¹⁶W. Götze and M. Lücke, *Phys. Rev. A* **11**, 2173 (1975); J. Bosse, W. Götze, and M. Lücke, *Phys. Rev. A* **17**, 434 (1978).
- ¹⁷R. Zwanzig, in *Lectures in Theoretical Physics*, edited by W. Brittin and L. Dunham (Wiley-Interscience, New York, 1961), Vol. 3, p. 135.
- ¹⁸H. Mori, *Prog. Theor. Phys.* **33**, 423 (1965); **34**, 399 (1965).
- ¹⁹P. C. Martin, in *Probleme a N Corps*, edited by C. De Witt and R. Balian (Gordon and Breach, New York, 1968), p. 37.
- ²⁰P. A. Egelstaff, *An Introduction to the Liquid State* (Academic, London, 1967).
- ²¹G. H. Vineyard, *Phys. Rev.* **110**, 999 (1958).
- ²²J. Bosse, W. Götze, and M. Lücke, *Phys. Rev. A* **17**, 447 (1978).
- ²³J. Bosse, W. Götze, and M. Lücke, *Phys. Rev. A* **18**, 1176 (1978).
- ²⁴A. Rahman, *Phys. Rev. A* **9**, 1667 (1974); *Phys. Rev. Lett.* **32**, 52 (1974).
- ²⁵J. L. Yarnell, M. J. Katz, and R. G. Wentzel, *Phys. Rev. A* **7**, 2130 (1973).
- ²⁶L. P. Kadanoff and P. C. Martin, *Ann. Phys.* **24**, 419 (1963).